

Analysis of third-grade heat absorption hydromagnetic exothermic chemical reactive flow in a Darcy-forchheimer porous medium with convective cooling

S.O. Salawu

**Department of Mathematics, Faculty of Physical Sciences, Landmark University,
Omu-aran, Nigeria.**

e-mail:kunlesalawu2@gmail.com

Abstract

The study examine boundary layer non-Newtonian fluid, laminar, viscous and incompressible heat absorption chemical reactive flow with asymmetry convective cooling in a Darcy-forchheimer porous medium. The electrically conducting fluid flow is driven by thermal buoyancy force and axial pressure gradient along a fixed channel. The convective exchange heat with the surrounding temperature at the walls surface follows Newtons law of cooling. The solutions to the dimensionless nonlinear equations governing the flow are obtained using weighted residual method (WRM). The computational assessment of the analytical results in the boundary layer is carried out and the graphical results for the momentum and energy distributions are obtained. The coefficient of skin friction and Nusselt number are also showed and discussed accordingly for some pertinent parameters entrenched in the flow. From the result shows that a rise in Frank-Kamenetskii parameter needs to be guide because it contribute significantly to the destruction of the system thermo-fluid also there is an increase in the fluid bonding force that makes it to be more viscoelastic as the non-Newtonian parameter increases.

Keywords: Hydromagnetic; Exothermic reaction; Darcy-forchheimer; Heat absorption; Convective cooling

1.0 Introduction

A porous medium is characterized by its porosity and other properties of the medium like tensile strength, tortuosity, electrical conductivity, permeability that can be obtained from their respective constituents properties (fluid and solid matrix), their pores structure and media porosity are habitually complex [1-3]. Darcy describes the flow past porous media that forms the scientific starting point of fluid permeability used in earth sciences, particularly in hydrogeology. This is a phenomenologically resulting from constitutive equation that illustrates the fluid flow past permeable media. For large velocities in a porous medium, inertial special effects can become significant. An inertial term is introduced to the Darcy's equation which is referred to as Forchheimer term. This term is able to account for the

nonlinear behavior of the pressure difference versus velocity data [4,5]. The idea of porous media is used in several practical areas of science and engineering such as filtration, geomechanics, bio-remediation, petroleum geology, material science, biophysics etc.

Studies associated with porous medium and flows of an electrically conducting fluid have fascinated many researchers because of their applications in numerous natural and technological processes. A review of magnetohydrodynamics (MHD) studies as related to technological fields was established by [6,7]. The basic influence of convective heat transfer in MHD was examined in [8,9]. While, [11,12] reported on Joule heating and viscous influences on hydromagnetic flow with heat transfer. Special weight was given to buoyancy forces on magnetohydrodynamics flow past a porous medium by [13,14]. The above cited

work never takes into account the likely effects of heat absorption. However, several processes in engineering happen at high temperatures and heat absorption along with difference in the fluid viscosity in design of some equipment [15].

Also, Theoretical study of non-Newtonian liquids has in present times attracted the attention of many researchers due to their industrial applications. Non-Newtonian fluids cannot be presented with single constitutive formulation, therefore the constitutive models for non-Newtonian fluid depends on the categories of fluids being considered which cannot be satisfactorily captured by the linearly viscoelastic classical model. Among the several constitutive equations include the class of third order fluids that cannot be solve analytically even for the simple form of the flows and therefore a computational technique is inevitable. Broad studies concerning the non-Newtonian fluids have been examined by [16-18]. In [19], investigation of overall thermodynamics, uniqueness and stability of the models for various kind of third grade fluid being an unusual instance involving heat balance was considered. Analysis relating to energy and species transfer in viscoelastic third grade fluids have been studied in [20]; nonetheless most of the research did not examine the thermodynamics aspect in relation to combined effects of non-Darcy, heat absorption, chemical kinetics and hydromagnetic of the flow system in a channel with convective cooling on the surfaces. However, the study of reactive fluids is very significant in understanding the heat transfer behaviour of hydrodynamic lubricants in engineering systems.

The goal of this research study is to examine the third grade chemical reactive hydromagnetic fluid flow with heat absorption in Darcy-forchheimer porous media between two fixed wall in the presence of a unvarying magnetic field and convective cooling. The mathematical model is presented in section 2. In section 3, the weighted residual technique is established and implemented for the solution process. In section 4, both the computational and graphical results are offered and quantitatively explained based on some existing fluid parameters entrenched in

the flow system.

2.0 Mathematical Formulation of the Model

Consider a convective cooling exothermic chemical reaction, laminar and incompressible third grade fluid flow through a non-Darcy porous parallel horizontal channel medium as presented in Figure 1. The non-Newtonian model is employed to produce the viscoelastic effects. The flow is induced by bimolecular chemical kinetics and assumed to be driven by both the axial pressure gradient and buoyancy force. The flow is assumed to be along x -axis with y -axis normal to the flow. The plate surfaces are subjected to exchange of heat with the ambient temperature. To simplify the model equations, the Maxwell equations of electromagnetism is neglected by supposing that the fluid has small electrical conductivity and therefore that a constant electromagnetic force is subsequently produced. In this case, the density variation is approximated according to the Boussinesq approximation.

Following [20,21], and ignoring the the fluid reactive viscose consumption, time-dependent effects and assumed low magnetic Reynolds number. The momentum and energy balance equations governing the flow are as follows:

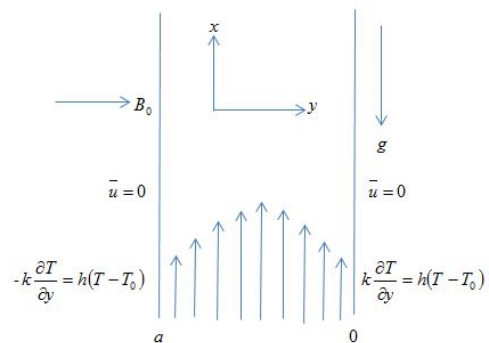


Figure 1. Geometry of the flow

$$-\frac{d\bar{P}}{dx} + \nu \frac{d^2\bar{u}}{dy^2} - \frac{\sigma B_0^2 u}{\rho} + 6\alpha \frac{d^2\bar{u}}{dy^2} \left(\frac{d\bar{u}}{dy} \right)^2 - \frac{\nu}{K^*} \bar{u} - \frac{b}{K^*} \bar{u}^2 + g\beta_T (T - T_0) = 0, \quad (1)$$

$$k \frac{d^2 T}{dy^2} + \left(\frac{d\bar{u}}{dy} \right)^2 \left[\nu + 2\alpha \left(\frac{d\bar{u}}{dy} \right)^2 \right] + QCA \left(\frac{KT}{\nu l} \right)^m e^{\frac{E}{RT}} - Q_0(T - T_0) + \frac{\sigma B_0^2}{\rho} \bar{u}^2 = 0 \quad (2)$$

The boundary conditions imposed takes the form:

$$\begin{aligned} \bar{y} = a; \quad \bar{u} = 0, \quad -k \frac{dT}{dy} &= h(T - T_0) \\ \bar{y} = 0; \quad \bar{u} = 0, \quad k \frac{dT}{dy} &= h(T - T_0). \end{aligned} \quad (3)$$

were \bar{u} , \bar{P} , T , T_0 , K^* , b , ν , ρ , l , β , g and α are respectively the fluid axial velocity, fluid pressure, fluid temperature, ambient temperature, Permeability of the porous medium, Forchheimer parameter of the medium, kinematic viscosity, density, channel width, expansivity coefficient, gravity and material coefficients. The terms k , Q , C , A , R , K , l , m , E , ν , Q_0 and h are the thermal conductivity, heat of reaction, species concentration, constant reaction rate, constant universal gas, Boltzmann's constant, Planck's number, numerical exponent, activation energy, vibration frequency, heat absorption coefficient and heat transfer coefficient respectively. Using the dimensionless quantities eqn. (4) on eqns. (1)-(3),

$$\begin{aligned} x = \frac{\bar{x}}{a}, \quad u = \frac{a\bar{u}}{\nu}, \quad \theta = \frac{E(T - T_0)}{RT_0^2}, \quad P = \frac{\bar{P}a^2}{\nu^2}, \\ F_s = \frac{ab}{K^*}, \quad D_a = \frac{a^2}{K^*}, \quad n = \frac{RT_0}{E}, \\ G = -\frac{dP}{dx}, \quad \beta = \frac{\alpha\nu}{a^4}, \quad Gr = \frac{a^3 g \beta RT_0^2}{\nu^2 E}, \\ \gamma = \frac{\nu^3 e^{\frac{E}{RT}}}{QAa^4 C} \left(\frac{\nu l}{RT_0} \right)^m, \quad y = \frac{\bar{y}}{a}, \quad Bi = \frac{ah}{K} \\ \delta = \frac{QE A a^2 C e^{\frac{E}{RT}}}{RKT_0^2} \left(\frac{KT_0}{\nu l} \right)^m, \\ \lambda = \frac{Q_0 T_0^2 R K e^{\frac{E}{RT}}}{E^2 QAC} \left(\frac{\nu l}{KT_0} \right)^m. \end{aligned} \quad (4)$$

Therefore, the governing equations transforms to:

$$G + \frac{d^2 u}{dy^2} - Ha^2 u + 6\beta \frac{d^2 u}{dy^2} \left(\frac{du}{dy} \right)^2 - D_a u - F_s u^2 + Gr\theta = 0, \quad (5)$$

$$\begin{aligned} \frac{d^2 \theta}{dy^2} + \delta(1 + n\theta)^m e^{\frac{\theta}{1+n\theta}} + \\ \gamma \left\{ Ha^2 u^2 + \left(\frac{du}{dy} \right)^2 \left[1 + 2\beta \left(\frac{du}{dy} \right)^2 \right] - \lambda \theta \right\} = 0. \end{aligned} \quad (6)$$

With boundary conditions as follows:

$$\begin{aligned} u = 0, \quad \frac{d\theta}{dy} = -Bi\theta \quad \text{at } y = 1 \\ u = 0, \quad \frac{d\theta}{dy} = Bi\theta \quad \text{at } y = 0. \end{aligned} \quad (7)$$

where G , Ha , β , D_a , F_s , Gr , δ , n , γ , λ and Bi parameter represent the pressure gradient, Hartmann number, non-Newtonian, Darcy, Forchheimer inertia number, thermal Grashof number, Frank-kamenetskii parameter, activation energy, viscous heating, heat

absorption and Biot number respectively.

3.0 Method of solution

The idea of weighted residual method see [22] is to look for an approximate result, in the polynomial form to the differential equation given as

$$D[v(y)] = f \text{ in the domain } R, \tag{8}$$

$$A_\mu[v] = \gamma_\mu \text{ on } \partial R.$$

where $D[v]$ represents a differential operator relating non-linear or linear spatial derivatives of the dependent variables v , f is the function of a known position, $A_\mu[v]$ denotes the

approximate number of boundary conditions with R been the domain and ∂R the boundary. By assuming an approximation to the solution $v(y)$, an expression of the form

$$v(y) \approx w(y, a_1, a_2, a_3 \dots a_n). \tag{9}$$

which depends on a number of parameters $a_1, a_2, a_3 \dots a_n$ and is such that for arbitrary value a_i 's the boundary conditions are satisfied and the residual in the differential equation become

$$E(y, a_i) = L(w(y, a_i)) - f(y). \tag{10}$$

The aim is to minimize the residual $E(y, a)$ to zero in some average sense over the domain. That is

$$\int_y E(y, a) W_i dy = 0, \quad i = 1, 2, 3, \dots n. \tag{11}$$

where the number of weight functions W_i is exactly the same with the number of unknown constants a_i in w . Here, the weighted functions are chosen to be Dirac delta functions. That is, $W_i(y) = \delta(y - y_i)$, such that the error is zero at the chosen nodes y_i . That is, integration of equation (11) with $W_i(y) = \delta(y - y_i)$ results in $E(y, a_i) = 0$.

By applying WRM to equations (5) to (7), assuming a polynomial with unknown coefficients or parameters to be determined later, this polynomial is called the trial function which are defined as follow:

$$u(y) = \sum_{i=0}^n a_i y^i, \quad \theta(y) = \sum_{i=0}^n b_i y^i. \tag{12}$$

By imposing the boundary conditions (7) on the trial functions (12) as well as substituting the trial functions into equations (5) and (6) to obtain the residual:

$$u_r = G + 90y^8 a_{10} + 72y^7 a_9 + 56y^6 a_8 + 42y^5 a_7 + 30y^4 a_6 + 20y^3 a_5 + 12y^2 a_4 + 6ya_3 + 2a_2 - Ha^2 \left(\begin{array}{l} y^{10} a_{10} + y^9 a_9 + y^8 a_8 + y^7 a_7 \\ + y^6 a_6 + y^5 a_5 + y^4 a_4 + y^3 a_3 \\ + y^2 a_2 + ya_1 + a_0 + \dots \end{array} \right) \tag{13}$$

$$\theta_r = 90y^8 b_{10} + 72y^7 b_9 + 56y^6 b_8 + 42y^5 b_7 + 30y^4 b_6 + 20y^3 b_5 + 12y^2 b_4 + 6yb_3 + 2b_2 + \delta \left(n \left(\begin{array}{l} y^{10} b_{10} + y^9 b_9 + y^8 b_8 + y^5 b_5 + y^7 b_7 + y^6 b_6 + y^4 b_4 + y^3 b_3 + y^2 b_2 + yb_1 + b_0 \end{array} \right) \right) + \dots \tag{14}$$

Minimizing the residual error to zero at some set of collocation points at a regular interval within the domain when

$$Gr = 0.2, m = 0.5, Bi = 1, n = 0.5, \beta = 0.2, Ha = 1, \lambda = 2, \gamma = 0.1, G = 0.5, Fs = 0.5, \delta = 0.5$$

and $Da = 0.5$. That is, $y_k = \frac{(b-a)k}{N}$ where

$k = 1, 2, \dots, N - 1$ and $a = 0, b = 1, N = 10$. The solution are obtained using MAPLE software.

Hence, the dimensionless momentum and energy equations becomes

$$u = -0.000050y^{10} + 0.000250y^9 - 0.000812y^8 + 0.001748y^7 + 0.000528y^6 - 0.006652y^5 - 0.004559y^4 + 0.021743y^3 - 0.264232y^2 + 0.252035y$$

$$\theta = 0.000003y^{10} - 0.000013y^9 + 0.000012y^8 + 0.000028y^7 - 0.000970y^6 + 0.002757y^5 + 0.009242y^4 - 0.023024y^3 - 0.331766y^2 + 0.343729y + 0.343729 \tag{15}$$

The procedure for weighted residual method is repeated for varying values of the embedded parameters. The other quantities of engineering interest are the skin friction (τ) and the wall heat transfer rate (Nu) defined as follows:

$$\tau = \frac{\partial u}{\partial y}, \quad Nu = -\frac{\partial \theta}{\partial y}$$

Table 1: Comparsim of results when $\beta = 0.01$, $G = 1$, $m = \gamma = n = 0.1$, $Bi = 10$, $Da = Fs = Gr = \delta = Ha = 0$,

y	[28] perturbation	[28] (ADM)	Present (WRM)
-1	0.000000	1.7130E-17	0.000000
-0.75	0.215486	0.215486	0.215486
-0.5	0.370497	0.370497	0.370497
-0.25	0.463957	0.463957	0.463956
0	0.495188	0.495188	0.495188
0.25	0.463957	0.463957	0.463961
0.5	0.370497	0.370497	0.370496
0.75	0.215486	0.215486	0.215486
1	0.000000	1.7130E-17	0.000000

4.0 Results and Discussion

To get a clear insight of the physical results, it is necessary to carry out computational study of the problem for the momentum field, energy field, the skin friction, and the thermal gradient number.

Table 1 shows the comparism of the present study to a special case of existing study. The existing analysis on the study under diverse method of solutions are in good agreement with the present technique of solution as presented in the table. The numerical results obtained using perturbation technique and Adomian decomposition method (ADM) in the previous

study are compared well with the present Weighted residual method (WRM) in the special case of the problem.

The reaction of varying in values of the thermal Grashof number Gr on the momentum profile is shown in Figure 2. It is noticed that a rise in the values of relative effect of the thermal buoyancy force to the viscous hydrodynamic force in the boundary layer causes an increase in the velocity distributions. This is due to the fact that the fluid flow get warmer as it moves through the channel within the boundary layer and thereby decreases the flow resistance forces that resulted in an enhancement in the fluid flow rate. For low buoyancy effects, the maximum flow velocity occurs. The energy profiles for variation in the numerical exponent m is presented in Figure 3. The heat rises with respect to an increase in the values of m from 0.2 to 1.0. The temperature measure the average rate of the kinetic energy possessed by the fluid particles and the higher the vibration of the particle, the more the fluid temperature increases. Therefore, heat is transported from the center line that increases the fluid average kinetic energy which leads to a rise in the temperature fields.

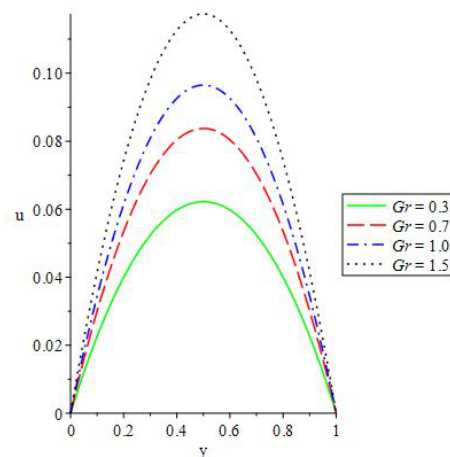


Figure 2. Effects of (G) on Velocity

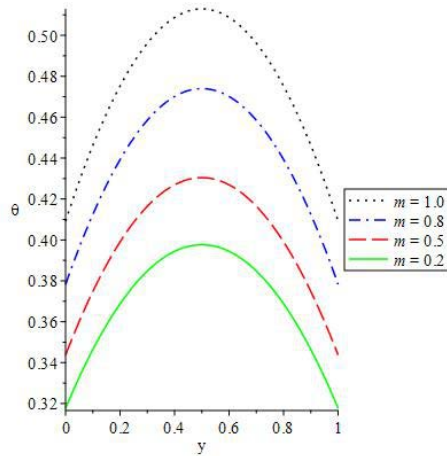


Figure 3. Effects of (m) on Temperature

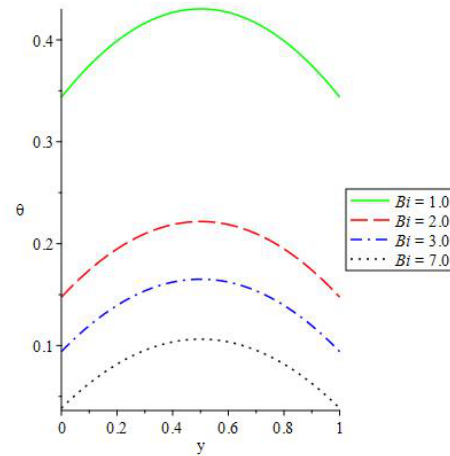


Figure 4. Effects of (Bi) on Temperature

Figure 4 depicts the consequence of Biot number Bi on the temperature fields. It is observed from the thermal boundary layer condition (7) that the higher the Biot number the greater the channel convective cooling that resulted in corresponding decrease in the surface temperatures and the bulk fluid. The entire system temperature diminish with a rise in the parameter values Bi as the liquid temperature continually modifies to the same temperature throughout the system. The reduction in the temperature increases the fluid viscosity that in turn retards the fluid momentum as the thermal boundary layer gets thinner. Figure 5 shows the effect of Hartmann number Ha on the flow profiles. It is seen that the velocity fields reduces with a rise in the magnetic field parameter Ha . The reduction in the profiles is due to an induced in the magnetic field in an electrically conducting fluid that stimulate a drag force known as Lorentz force which resists the fluid motion as shown in the figure. As a result of the opposition to the fluid motion due to Lorentz force, an additional extra work is done that changes the thermal energy.

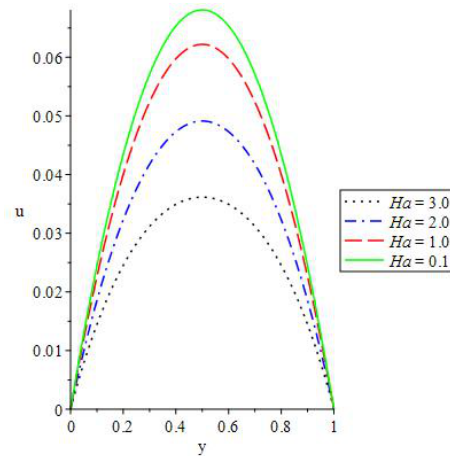


Figure 5. Effects of (Ha) on Velocity

Figure 6 demonstrates the heat profiles for diverse values of the heat absorption parameter λ . The result portray that an increase in the values of λ causes a decrease in the energy distributions as expected. This is because heat is able to leave the system as the exothermic chemical reaction takes place within the channel thereby reduces the thermal boundary layer thickness as a result, more heat diffused out of the system and causes decrease in the temperature profile. Figure 7 represents the influence of variations in pressure gradient G on fluid momentum. An increase in the parameter values G results in an increase in the fluid velocity i.e. a maximum velocity is achieved as the pressure gradient rises which mean that the greater the pressure apply on the fluid in the channel, the faster the viscoelastic liquid flow.

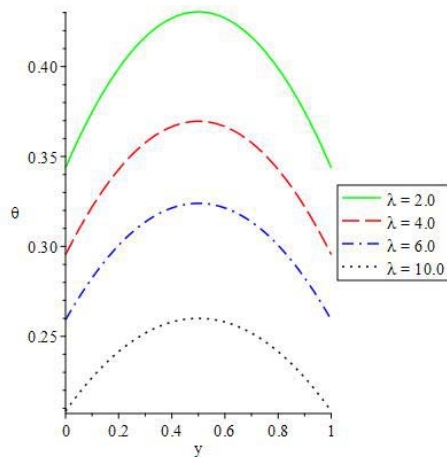


Figure 6. Effects of (λ) on Temperature

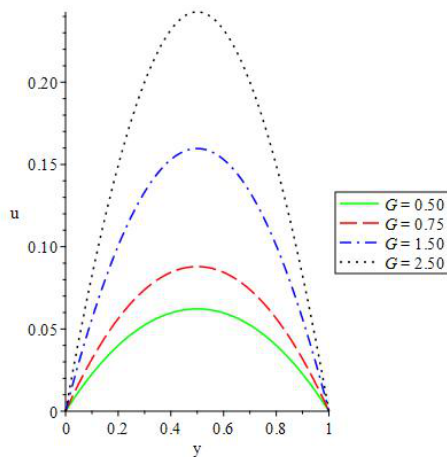


Figure 7. Effects of (G) on Velocity

Figure 8 portrays the response of viscoelastic parameter β on the velocity distribution. From the figure, it is seen that an increase in the non-Newtonian parameter reduces the fluid flow rate. This is due to an increase in the fluid particle bonding force that makes the fluid to be more viscoelastic. Therefore, the fluid momentum distribution in the system diminishes. The descending trend is due to the imbalance between the convective cooling and nonlinear heat at the surfaces as the viscoelastic parameter increases.

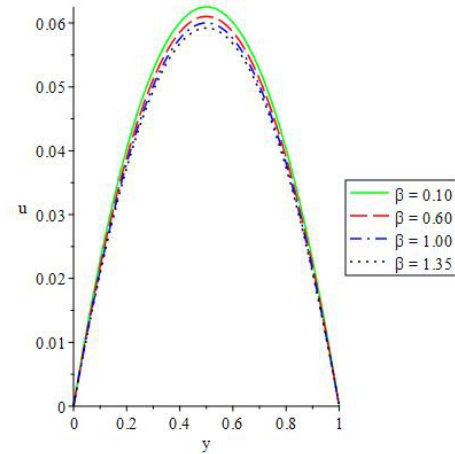


Figure 8. Effects of (β) on Velocity

Figures 9 and 10 illustrate the effects of the Darcy and Forchheimer parameters Da and Fs respectively on the velocity profiles. It is noticed from the figures that the velocity profiles decrease with an increase in the values of Da or Fs respectively. This is due to the fact that the porosity parameters introduces a linear or second order quadratic drag into the fluid in the channel by causing a reduction in the flow velocity rate within the boundary layer which then reduces the velocity distribution.

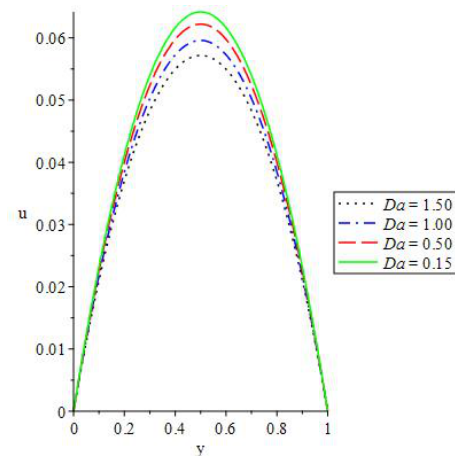


Figure 9. Effects of (Da) on Velocity

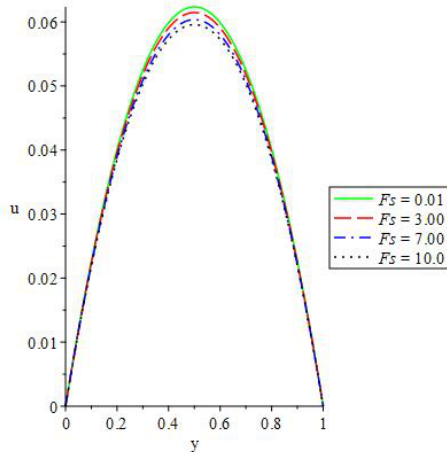


Figure 10. Effects of (F_s) on Velocity

Figure 11 represents the reaction of the temperature to variational increase in the Frank-Kamenetskii parameter δ . The figures show that an increase in the reaction parameter enhances energy rate in the channel. That is, the internal heat generation rises as the reacting reagents is enhances. The exothermic chemical reaction increases the heat transfer rate from the combustion region to the cooling surface. Furthermore, heat is transfer over the fluid to melt the fluid viscosity in other to raise the collision of particles; similarly, extra heat is generated by the interaction of viscous fluid particle that in turn increases the profile.

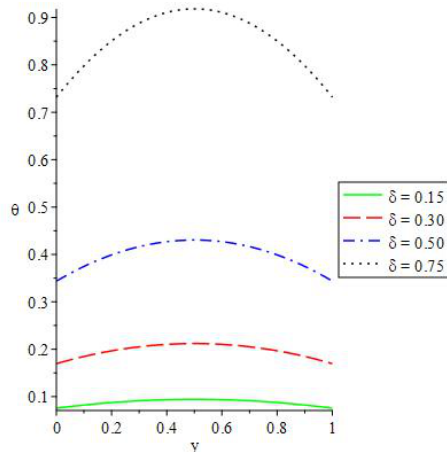


Figure 11. Effects of (δ) on Temperature

The responses of the skin friction to an increase in the parameter values Ha and G respectively are illustrated in the Figures 12 and 13. It is observed that the skin friction initially decreases

as magnetic field parameter values Ha increases but increases as it move far away from the boundary surface while an opposite effect is noticed when the pressure gradient term G is enhanced. The skin friction rises within the range $0 \leq y \leq 0.5$ and reduces within the range $0.5 \leq y \leq 1$ as the value of G increases.

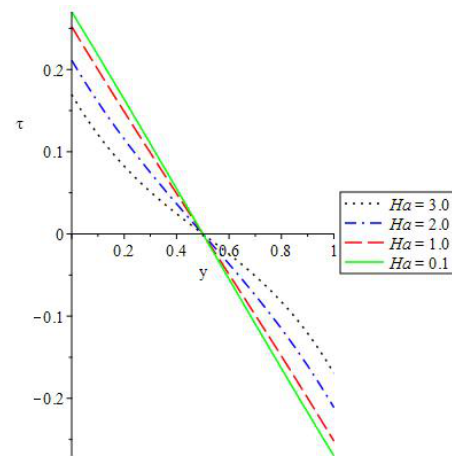


Figure 12. Effects of (Ha) on Skin friction

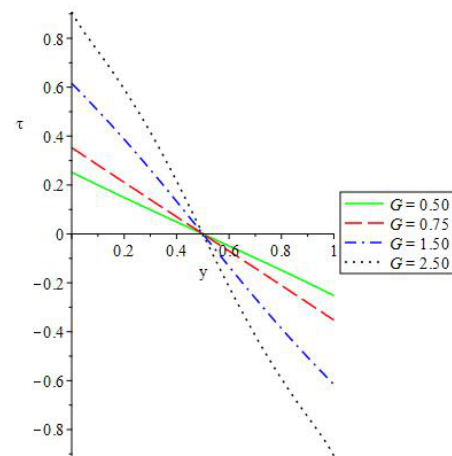


Figure 13. Effects of (G) on Skin friction

The thermal gradient effect initially increases and later decreases as it move distance away from the wall as the Frank-Kamenetskii parameter δ rise as displayed in Figure 14 as a result of respective increase and reduction in the thermal boundary layers. While a converse effect is experienced when the values of the heat absorption is increases. From the figure, a early reduction in the effect is noticed but later

increases as it keep distance from the boundary wall in the rang $0.5 \leq y \leq 1$ as presented in Figure 15 at $y \rightarrow 1$.

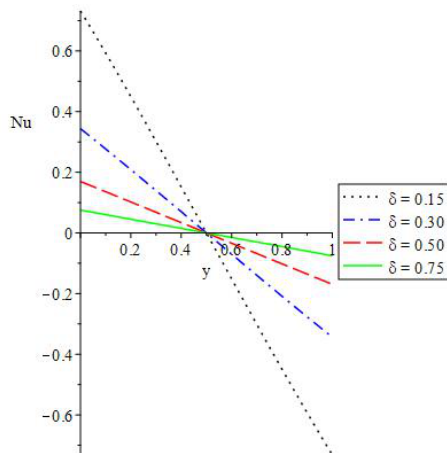


Fig. 14. Effects of (δ) on Nusselt number

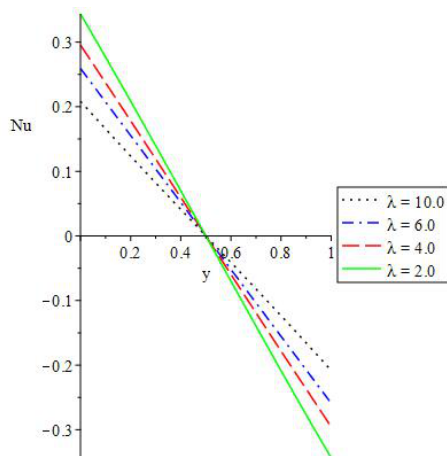


Figure 15. Effects of (λ) on Nusselt number

5.0 Conclusion

The influences of heat transfer on third grade exothermic chemical reactive fluid flow past a non-Darcy porous medium with heat absorption have been studied. The formulated equations for the flow are non-dimensionalised and solved using a weighted residual method (WRM) to get the velocity and temperature distribution as well as the skin friction and Nusselt number. Calculated results are represented graphically to show the important of some parameters on the flow. It is observed that:

(i) a rise in Frank-Kamenetskii parameter needs to be guide because it contribute significantly to the destruction of the system thermo-fluid while

the Darcy and Forchheimer parameters resist the free flow of viscoelastic fluid profile.

(ii) An increase in heat absorption and Biot number retards temperature distribution and increases the fluid bonding force that result in slow movement of the non-Newtonian liquid.

(iii) An increase in the viscoelastic of the fluid has a significant effects on the flow fluid.

Reference

- [1] T. Dutta, Fractal pore structure of sedimentary rocks: Simulation by ballistic deposition, *Journal of Geophysical Research: Solid Earth*, (2003), pp.108.
- [2] M. K. Head, H. S. Wong and N. R., Buenfeld, Characterisation of 'Hadley' Grains by Confocal Microscopy, *Cement & Concrete Research*, Vol. 36, No. 8, (2006), pp.1483-1489.
- [3] S. Peng, Q. Hu, S. Dultz and M. Zhang, Using X-ray computed tomography in port structure characterization for Berea sandstone: Resolution effect, *Journal of Hydrology*, (2012), pp.254-261.
- [4] S. O. Salawu and M. S. Dada, Radiative heat transfer of variable viscosity and thermal conductivity effects on inclined magnetic field with dissipation in a non-Darcy medium, *Journal of the Nigerian Mathematical Society*, Vol. 35, (2016), pp.93-106 .
- [5] R. A. Kareem and S. O. Salawu, Variable viscosity and thermal conductivity effect of sores and dufour on inclined magnetic field in non-Darcy permeable medium with dissipation, *British Journal of Mathematics & Computer Science*, Vol. 22, No. 3, (2017), pp.1-12
- [6] R. Moreau, *Magnetohydrodynamics*, Dordrecht: Kluwer Academic Publishers. (1990).
- [7] M. G. Reddy and N. Sandee, computational modelling and analysis of heat and mass transfer in MHD flow past the upper part of a paraboloid of revolution", *Eur. Phys. J. Plus*, 132: 222, (2017).
- [8] O. D. Makinde and T. Chinyoka, Numerical investigation of transient heat

- transfer to hydromagnetic channel flow with radiative heat and convective cooling, *Commun Nonlinear Sci Numer Simulat*, Vol. 15, (2010), pp.3919-3930.
- [9] M. A. Hossain, Viscous and Joule heating effects on MHD free convection flow with variable plate temperature, *Int J Heat Mass Transfer*, Vol. 35, (1992), pp.3485.
- [10] M. G. Reddy and N. Sandeep, Free convective heat and mass transfer of magnetic bio-convective flow caused by a rotating cone and plate in the presence of nonlinear thermal radiation and cross diffusion, *Journal of Computational and Applied Research in Mechanical Engineering*, Vol.7, (2017), pp. 1-21.
- [11] S. O. Salawu and E. O. Fatunmbi, Dissipative heat transfer of micropolar hydromagnetic variable electric conductivity fluid past inclined plate with Joule heating and non-uniform heat generation, *Asian Journal of Physical and Chemical Sciences*, Vol. 2, (2017), pp.1-10.
- [12] O. D. Makinde and P. Sibanda, Magnetohydrodynamic mixed convective flow and heat and mass transfer past a vertical plate in a porous medium with constant wall suction”, *Trans ASME – J Heat Transfer*, Vol. 130, (2008), pp.602-610.
- [13] M. G. Reddy, Heat and mass transfer on magnetohydrodynamic peristaltic flow in porous media with partial slip, *Alexandria Engineering Journal*, Vol. 55, (2016), pp. 1225–1234.
- [14] V. Ravikumar, M. C. Raju and G. S. S. Raju, Combined effects of heat Absorption and MHD on convective Rivlin-Ericksen flow past a semi-infinite vertical porous plate with variable temperature and suction, *Ain Shams Engineering Journal*, Vol. 5, (2014), pp.867-875.
- [15] S. Asghar, K. Hanif and T. Hayat, Flow of a third grade fluid due to an Accelerated disk, *International Journal for Numerical Methods in Fluids*, Vol. 63, No. 8, (2010), pp.887-902.
- [16] T. Hayat, E. Momoniat and F. M. Mahomed, Peristaltic MHD flow of third grade fluid with an endoscope and variable viscosity”, *Journal of Nonlinear Mathematical Physics*, Vol. 15, No. 1, (2008), pp.91-104.
- [17] O. D. Makinde, Thermal stability of a reactive third grade fluid in a cylindrical pipe: an exploitation of Hermite-Padé approximation technique, *Applied Mathematics and Computation*, Vol. 189, (2007), pp.690-697.
- [18] K. R. Rajagopal, *Boundary conditions for fluids of the differential type: Navier–stokes equations and related non-linear problems*, Plenum Press, New York, 273, (1995).
- [19] O. D. Makinde and T. Chinyoka, Numerical study of unsteady hydromagnetic generalized couette flow of a reactive third-grade fluid with asymmetric convective cooling, *Computers and Mathematics with Applications*, Vol. 61, (2011), pp.1167-1179.
- [20] T. Chinyoka and O. D. Makinde, Analysis of transient Generalized Couette flow of a reactive variable viscosity third-grade liquid with asymmetric convective cooling”, *Mathematical and Computer Modelling* Vol. 54, (2011), pp.160–174.
- [21] S. O. Adesanya, J.A. Falade, S. Jangili, O. Anwar Be’ g, Irreversibility analysis for reactive third-grade fluid flow and heat transfer with convective wall cooling, *Alexandria Engineering Journal*, Vol. 56, (2017), pp. 153–160.
- [22] M. S. Dada, and S. O. Salawu, Analysis of heat and mass transfer of an inclined magnetic field pressure-driven flow past a permeable plate”, *Appl. Appl. Math.*, Vol. 12, No. 1, (2017), pp.189-200.